Magnetic order in $Pr_2Pd_3Ge_5$ and possible heavy-fermion behavior in $Pr_2Rh_3Ge_5$

V. K. Anand and Z. Hossain*
Department of Physics, Indian Institute of Technology, Kanpur 208016, India

C. Geibel
Max Planck Institute for Chemical Physics of Solids, 01187 Dresden, Germany

(Received 18 June 2007; revised manuscript received 24 February 2008; published 5 May 2008)

We report our results on two ternary intermetallic compounds $Pr_2Pd_3Ge_5$ and $Pr_2Rh_3Ge_5$ based on magnetic susceptibility, magnetization, specific heat, resistivity, and magnetoresistance data. These compounds form in $U_2Co_3Si_5$-type orthorhombic structure (space group *Ibam*). $Pr_2Pd_3Ge_5$ exhibits two magnetic transitions at $T_{N1}=7.5$ K and $T_{N2}=8.3$ K. In the magnetically ordered state, $Pr_2Pd_3Ge_5$ exhibits a field-induced metamagnetic transition and unusually large magnetoresistance. $Pr_2Rh_3Ge_5$ does not show any phase transition down to 0.5 K. It has a crystal electric field singlet ground state, separated from the first excited state by about 10 K. The low lying crystal field excitations lead to exciton mediated electronic mass enhancement, as evidenced by a large Sommerfeld coefficient ($\gamma \sim 80$ mJ/mol K^2) in $Pr_2Rh_3Ge_5$.

DOI: 10.1103/PhysRevB.77.184407 PACS number(s): 75.47.De, 71.70.Ch, 71.27.+a, 75.30.Kz

I. INTRODUCTION

With the advent of unconventional heavy-fermion superconductivity in $PrOs_4Sb_{12}$, the Pr-based compounds have evolved as a topic of current interest in condensed matter physics.[1–4] Ce compounds present many examples of Kondo lattice and/or heavy-fermion behavior and magnetically mediated unconventional superconductivity, which occurs in the magnetic-nonmagnetic boundary. In contrast, so far we know of only one example of Pr-based heavy-fermion superconductor. The physics of heavy-fermion behavior in Pr compounds is very different from that in Ce compounds. While in Ce compounds, the heavy-fermion behavior has its origin in Kondo effect, in Pr compounds it is realized either due to the quadrupolar Kondo effect as in $PrInAg_2$,[5] or due to the excitonic mass enhancement as observed in $PrOs_4Sb_{12}$.[6] Both the routes of heavy-fermion behavior in Pr compounds critically depend on the crystal electric field (CEF) split ground state. The magnetic and transport properties of Pr compounds are strongly influenced by the crystal electric field effect. Exciting phenomena are observed in the Pr-based systems with nonmagnetic singlet and/or doublet ground state when the crystal field splitting energy becomes comparable with other interactions. Realizing that the Pr-based compounds can also present extraordinary magnetic and superconducting properties, we have started working on these systems with an objective of finding interesting Pr compounds and explore the interplay of magnetism and superconductivity in them. In order to achieve the destined goal, we are investigating $Pr_2T_3Ge_5$ compounds (T=transition elements) in view of interesting features of their Ce analogs. For example, $Ce_2Ni_3Ge_5$, which is a Kondo lattice antiferromagnetic system, exhibits pressure-induced superconductivity around 3.9 GPa.[7,8] Very recently, we investigated its Pr analog, $Pr_2Ni_3Ge_5$, and found an antiferromagnetic ordering below 8.5 K and two field-induced metamagnetic transitions as well as very high positive magnetoresistance in the ordered state.[9] In this paper, we report our findings on magnetic and transport properties of $Pr_2Pd_3Ge_5$ and $Pr_2Rh_3Ge_5$. Ce analogs of these two compounds, viz., $Ce_2Pd_3Ge_5$ orders antiferromagnetically at 3.8 K,[10] and $Ce_2Rh_3Ge_5$ is a moderate heavy-fermion antiferromagnet system.[11] The homologous compound $Pr_2Rh_3Si_5$ does not magnetically order down to 1.8 K due to the nonmagnetic singlet CEF ground state.[12]

II. EXPERIMENT

We prepared polycrystalline samples of $Pr_2Pd_3Ge_5$ and $Pr_2Rh_3Ge_5$ and the nonmagnetic La analogs starting with high purity elements in stoichiometric ratio by the conventional arc melting on a water cooled copper hearth under argon atmosphere. During the arc melting process, samples were flipped and remelted several times to improve the homogeneity. Arc melted samples were annealed at 1000 °C under vacuum for 7 days. Both annealed and as-cast samples were characterized by Cu K_α x-ray diffraction and scanning electron microscopy equipped with energy dispersive x-ray analysis (EDAX). Magnetization was measured using a commercial superconducting quantum interference device magnetometer. Resistivity was measured using a standard four probe ac technique. Heat capacity was measured using relaxation method in a physical property measurement system (PPMS-Quantum design). A second batch of Pr samples was also prepared to check for the reproducibility of the results.

III. RESULTS AND DISCUSSION

X-ray diffraction data on powdered samples of $R_2T_3Ge_5$ (R=Pr,La; and T=Pd,Rh) were analyzed using the software WINXPOW. These compounds crystallize in $U_2Co_3Si_5$-type orthorhombic structure (space group *Ibam*). The lattice parameters and unit-cell volumes are listed in Table I. $Pr_2Pd_3Ge_5$ and $Pr_2Rh_3Ge_5$ have slightly lower lattice volumes compared to their Ce analogs, and the lattice parameters of La compounds are in agreement with the reported values.[10,11] Powder x-ray diffraction and scanning electron micrographs revealed the samples to be essentially single phase [impurity phase(s) less than 3%]. EDAX composition

TABLE I. Lattice parameters and unit-cell volumes of orthorhombic (*Ibam*) system $R_2T_3Ge_5$ (R=Pr, La and T=Pd, Rh).

Compounds	a(Å)	b(Å)	c(Å)	V(Å^3)
$Pr_2Pd_3Ge_5$	10.150	12.084	6.144	753.6
$La_2Pd_3Ge_5$	10.186	12.223	6.182	769.6
$Pr_2Rh_3Ge_5$	10.078	12.091	5.978	728.4
$La_2Pd_3Ge_5$	10.149	12.185	6.033	746.1

analysis revealed the samples to have the expected 2:3:5 compositions.

A. $Pr_2Pd_3Ge_5$

Figure 1 shows the temperature dependence of magnetic susceptibility of $Pr_2Pd_3Ge_5$ at 1.0 T. The low temperature susceptibility data at different fields are shown in the inset of Fig. 1. At low fields (0.01 T), two well pronounced transitions are observed in the magnetic susceptibility data at 8.3 and 7.5 K. On increasing the strength of the applied field, both anomalies merge together and the peak position shifts to lower temperature (e.g., to 7.2 K at 1.5 T), which evidence the onset of an antiferromagnetic ordering at 8.3 K. At a field of 3 T and above, the susceptibility curve shows a tendency to saturation. The magnetic susceptibility follows the modified Curie–Weiss behavior $\chi=\chi_0+C/(T-\theta_p)$. At 1 T, the susceptibility data above 50 K fit nicely with $\chi_0=-8\times10^{-5}$ emu/Pr mole and the paramagnetic Curie–Weiss temperature $\theta_p=-6.1$ K. The effective moment $\mu_{\text{eff}}=3.53\mu_B$ is very close to the theoretically expected value for Pr^{3+} ions ($3.58\mu_B$).

From the isothermal magnetization data of $Pr_2Pd_3Ge_5$ shown in Fig. 2, we observe a rapid increase in magnetization at 1.6 T at low temperatures (2 K, which is well below

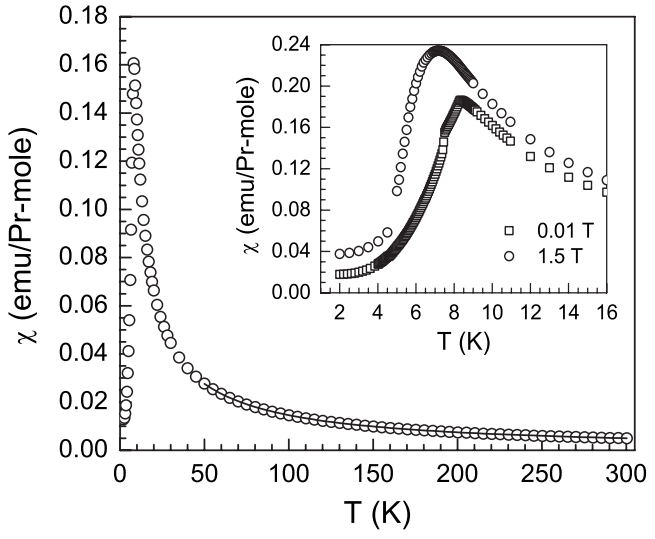

FIG. 1. The temperature dependence of magnetic susceptibility of $Pr_2Pd_3Ge_5$ at 1.0 T. The solid line represents the fit to the modified Curie–Weiss behavior. The inset shows the low temperature magnetic susceptibility data at two different fields.

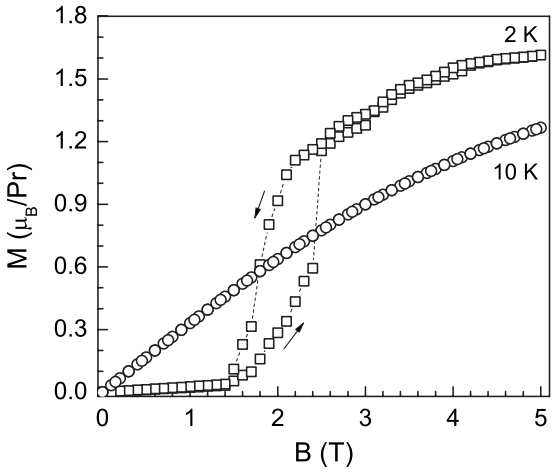

FIG. 2. Isothermal magnetization of $Pr_2Pd_3Ge_5$ as a function of field at temperatures of 2 and 10 K.

T_N) due to the occurrence of field-induced metamagnetic transition. This field-induced transition is accompanied by a large hysteresis. A slight nonlinearity in magnetization curve is found at 10 K, which is just above the magnetic ordering temperature. This may result from the presence of short range order above the magnetic ordering temperature and/or due to a contribution from the crystal electric field effect. At higher temperatures, magnetization exhibits a linear field dependence. In the ordered state, saturation magnetization is $1.65\mu_B$/Pr at 5 T.

Figure 3 shows the magnetic contribution to the specific heat of $Pr_2Pd_3Ge_5$, which we estimated by subtracting the specific heat of the nonmagnetic compound $La_2Pd_3Ge_5$ from the specific heat of $Pr_2Pd_3Ge_5$, assuming the lattice contribution to be roughly equal to that of $La_2Pd_3Ge_5$. The specific heat data of $La_2Pd_3Ge_5$ do not show any anomaly down to 2

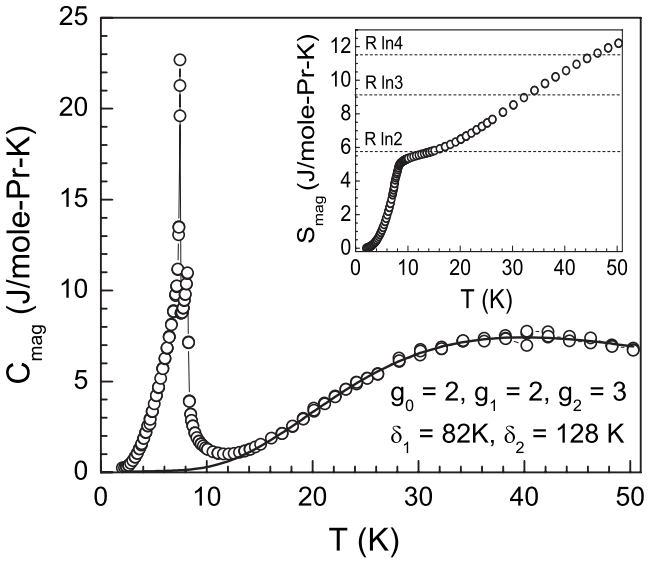

FIG. 3. Magnetic part of the specific heat of $Pr_2Pd_3Ge_5$. The solid line represents the fit to the three level CEF scheme, as described in the text. The inset shows the magnetic contribution to the entropy as a function of temperature.

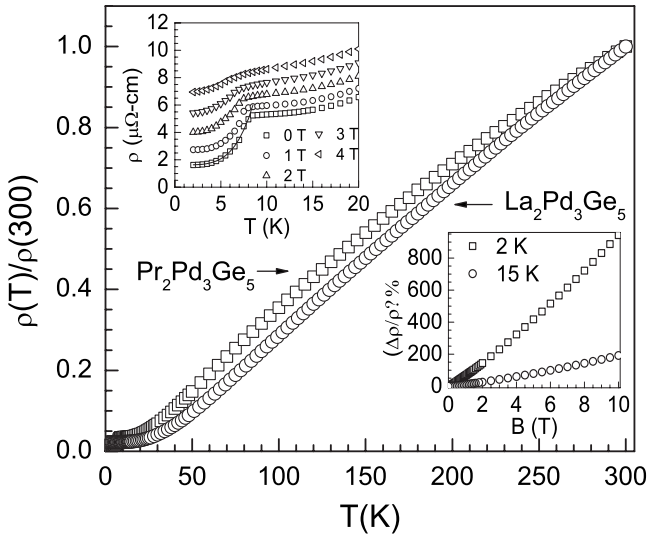

FIG. 4. Normalized electrical resistivity of $La_2Pd_3Ge_5$ and $Pr_2Pd_3Ge_5$ as a function of temperature in the temperature range 2–300 K. The upper inset shows the low temperature resistivity of $Pr_2Pd_3Ge_5$ at different fields, and the lower inset shows the magnetoresistance at 2 and 15 K. The solid line in the upper inset represents the fit to gapped magnon behavior in the ordered state.

K and has a γ value of ~5 mJ/La mole K^2 (below 10 K). The specific heat data of $Pr_2Pd_3Ge_5$ exhibit two sharp λ-type anomalies at 8.2 and 7.5 K, which confirm the intrinsic nature of magnetic ordering observed in magnetic susceptibility data. The anomaly at 7.5 K in specific heat is more pronounced in contrast to that in magnetic susceptibility. The specific heat data fit very nicely to the expression $C=\gamma T+\beta T^3 \exp(-E_g/k_BT)$ in the temperature range 2–7 K. This clearly means that the magnon spectrum has an energy gap in antiferromagnetic state, which, in turn, suggests the possibility of anisotropic magnetic behavior in this compound. The coefficients $\gamma=14$ mJ/Pr mole K^2 and $\beta=0.059$J/Pr mole K^4, and the energy gap $E_g=0.25$ meV.

At higher temperatures, the magnetic part of specific heat shows a Schottky-type anomaly in the form of a broad peak centered around 40 K. The experimentally observed magnetic specific heat data above 20 K could be reproduced by the crystal field scheme involving three levels: a doublet ground state separated by 82 K from a doublet first excited state and 128 K from the triplet second excited state. The solid line in Fig. 3 represents this CEF scheme and includes an additional electronic contribution with γ ~10 mJ/Pr mole K^2 (over that of $La_2Pd_3Ge_5$, which we subtracted while estimating the magnetic contribution to the specific heat). The magnetic contribution to the entropy attains a value of 5.35 J/Pr mole K at 10 K, which is 93% of R ln 2.

The results on electrical resistivity measurements of $La_2Pd_3Ge_5$ and $Pr_2Pd_3Ge_5$ are shown in Fig. 4. The resistivity data of $La_2Pd_3Ge_5$ have almost linear temperature dependence with a residual resistivity of ~4.5 $\mu\Omega$ cm at 2 K and residual resistivity ratio ~44. In the case of $Pr_2Pd_3Ge_5$, residual resistivity at 2 K is ~1.6 $\mu\Omega$ cm and residual resistivity ratio ~90. The low residual resistivities and high residual resistivity ratios indicate our polycrystalline samples to be of very good quality. The resistivity data of $Pr_2Pd_3Ge_5$ exhibit slight nonlinearity, which we attribute to crystal field effect. At low temperatures (below 15 K), the resistivity attains a nearly constant value before it undergoes a transition at T_N below which there is a sharp drop of resistivity due to reduction in spin disorder scattering. The low temperature resistivity data of $Pr_2Pd_3Ge_5$ at different magnetic fields up to 4 T are shown as inset in Fig. 4. With the increase in field strength, the resistivity anomaly due to phase transition starts to broaden and the value of residual resistivity increases, as is expected for an antiferromagnetic system.

The low temperature electrical resistivity data are described well by the following expression:[13]

$$\rho(T)=\rho_0+C\left\{\tfrac{1}{5}T^5+\Delta T^4+\tfrac{5}{3}\Delta^2T^3\right\}\exp(-\Delta/T),$$

where ρ_0 is the residual resistivity, C is the coefficient to the magnon contribution, and Δ is the magnon energy gap. The experimentally observed data are reproduced very accurately by the above expression in the temperature range 2–7 K with $\rho_0=1.62$ $\mu\Omega$ cm, $C=0.000\,17$ $\mu\Omega$ cm/K^5, and the energy gap $\Delta=3.40$ K. This is in accordance with the antiferromagnetic magnon gap-like feature observed in the specific heat data.

The lower inset of Fig. 4 shows the field dependence of resistivity at 2 and 15 K plotted as magnetoresistance $(\Delta\rho/\rho(0)=[\rho(B)-\rho(0)]/\rho(0)$, where $\rho(B)$ is the resistivity measured at a magnetic field B). A linear field dependence of resistivity is inferred both in the paramagnetic and antiferromagnetic states. The magnetoresistance is unusually high and positive in the ordered state. We observe almost ten times increase in resistivity at a field of 10 T at 2 K, which leads to a magnetoresistance of ~940%, which is surprisingly large. Even in the paramagnetic state, a large positive magnetoresistance is observed (~190% at 10 T at 15 K). Such a large positive magnetoresistance in an antiferromagnetically ordered polycrystalline intermetallic system is quite unusual and intriguing. Since isothermal magnetization in the ordered state shows metamagnetic transition at 1.6 T, one would expect a negative magnetoresistance in the vicinity of that characteristic field. However, no such effect is observed in transverse magnetoresistance (magnetic field perpendicular to current). This might be due to the fact that a large part of the resistance change is due to a modification of the trajectory of the current carrying electrons rather than changes in the electronic density of states (closing of superzone gap, etc.) by the application of magnetic field.

A large positive magnetoresistance (as high as 85%) has also been observed in antiferromagnetically ordered system $R_2Ni_3Si_5$ (R=Tb,Sm,Nd),[14] where it was suggested that such behavior could be the result of layered structure of rare-earth atoms, which provides the sheets of ordered spins in analogy with that in Dy/Sc superlattice.[15] A similar favorable situation also exists in the case of our compound $Pr_2Pd_3Ge_5$, which consists of layers of Pr atoms separated by Pd-Ge network in *Ibam* structure. Therefore, as in the case of $R_2Ni_3Si_5$ (R=Tb,Sm,Nd), the large positive giant magnetoresistance in $Pr_2Pd_3Ge_5$ may be speculated to arise from the layered nature of structure. We wish to emphasize here

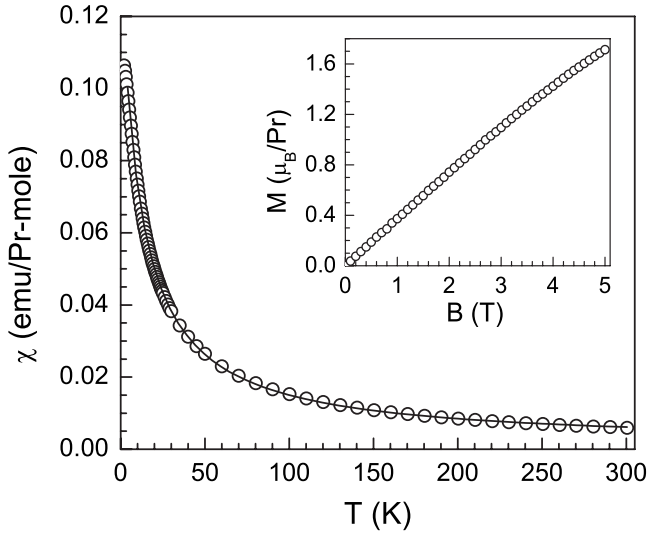

FIG. 5. Temperature dependence of magnetic susceptibility of $Pr_2Rh_3Ge_5$ at 0.1 T. The solid line represents the fit to the modified Curie–Weiss behavior. The inset shows the field dependence of isothermal magnetization at 2 K.

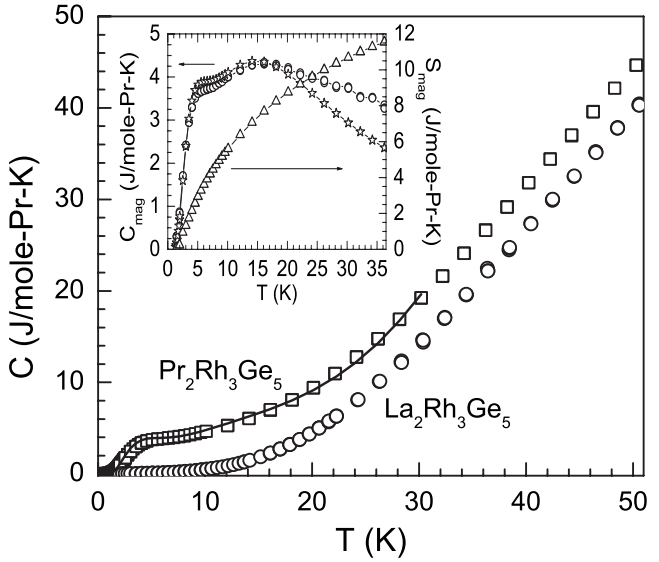

FIG. 6. Temperature dependence of the specific heat of $La_2Rh_3Ge_5$ and $Pr_2Rh_3Ge_5$ in the temperature range 0.5–50 K. The solid line is the fit to the CEF scheme, as described in the text. The inset shows the magnetic part of the specific heat and entropy as a function of temperature. The data shown by stars in the inset represent the magnetic part to the fit in CEF analysis.

that the magnitude of the magnetoresistance is exceptionally large and might have strong technological relevance. Such a high value (in excess of 200%) of magnetoresistance is observed in ballistic Ni nanocontacts.[16] An extremely large value of magnetoresistance (resistance decreases by a factor of 200) was also found in $HgCr_2Se_4$, which is caused by magnetic-field-induced changes in the carrier mobility and concentration.[17]

Apart from the unusually large magnetoresistance, the sharp drop of magnetization below 7.5 K, the sharp increase in magnetization above the critical field, and the gapped behavior in the specific heat and resistivity are strong indications of a strongly anisotropic Ising-type antiferromagnetic system. Investigations on single crystals are desired to further understand the anisotropic magnetic properties of this compound.

B. $Pr_2Rh_3Ge_5$

The magnetic susceptibility data of $Pr_2Rh_3Ge_5$ at a field of 0.1 T are plotted in Fig. 5. The susceptibility curve is found to obey the modified Curie–Weiss behavior without any magnetic ordering down to 2 K. From a fit to the susceptibility data above 7 K with $\chi=\chi_0+C/(T-\theta_p)$, we obtained $\chi_0=1.18\times10^{-3}$ emu/Pr mole and the paramagnetic Curie–Weiss temperature $\theta_p=-11.5$ K. The effective moment μ_{eff} came out to be $3.51\mu_B$, which is very close to the theoretical value of $3.58\mu_B$ for Pr^{3+}. The isothermal magnetization data at 2 K (shown in the inset of Fig. 5) show almost linear field dependence, which is a characteristic of a paramagnetic system, and the magnetization does not reach to saturation value up to 5 T field.

The specific heat data of $La_2Rh_3Ge_5$ and $Pr_2Rh_3Ge_5$ are plotted in Fig. 6. No anomaly is observed in the specific heat data of $La_2Rh_3Ge_5$ down to 2 K, and the γ value is estimated to be $\sim$10 mJ/La mole K^2. In the case of $Pr_2Rh_3Ge_5$, the specific heat data do not also exhibit any pronounced anomaly due to a phase transition. We, however, notice a broad Schottky-type peak centered around 4.5 K. The solid line in Fig. 6 represents the crystal field analysis and includes a phonon contribution equal to that of $La_2Rh_3Ge_5$ and an additional electronic contribution to take care for the difference in Sommerfeld coefficients of $La_2Rh_3Ge_5$ and $Pr_2Rh_3Ge_5$. The magnetic contribution to the specific heat of $Pr_2Rh_3Ge_5$, which was estimated as the difference in the specific heats of $Pr_2Rh_3Ge_5$ and $La_2Rh_3Ge_5$, is shown in the inset of Fig. 6 together with the magnetic entropy and the crystal field analysis. The experimentally observed magnetic specific heat data at low temperatures are fairly reproduced by the four low lying crystal electric field levels (four CEF singlets at 0, 12, 40, and 60 K) with a significant departure above 20 K due to the contribution from higher excited states. That the ground state is a singlet separated by 12 K from the first excited is further supported from the fact that magnetic entropy attains a value of R ln 2 at 10 K (inset of Fig. 6). The temperature dependence of magnetic entropy also reveals the significant contribution from higher excited states, e.g., an increased value of magnetic entropy over R ln 3 at 40 K is due to the contribution from the levels above 40 K. Furthermore, a constant difference in the specific heats of $Pr_2Rh_3Ge_5$ and $La_2Rh_3Ge_5$, which starts appearing above 25 K, is an indication of the involvement of closely spaced excited states. From such a behavior of the specific heat, we can suggest that in this case the crystal field possibly removes the ninefold degeneracy of Pr^{3+} by splitting them into nine singlets, which is expected in the orthorhombic environment. This CEF split nonmagnetic singlet ground state leads to no magnetic ordering in $Pr_2Rh_3Ge_5$. In the case of homologous compound $Pr_2Rh_3Si_5$ too, after an analysis of crystalline electric field, Ramakrishnan *et al.* suggested a sin-

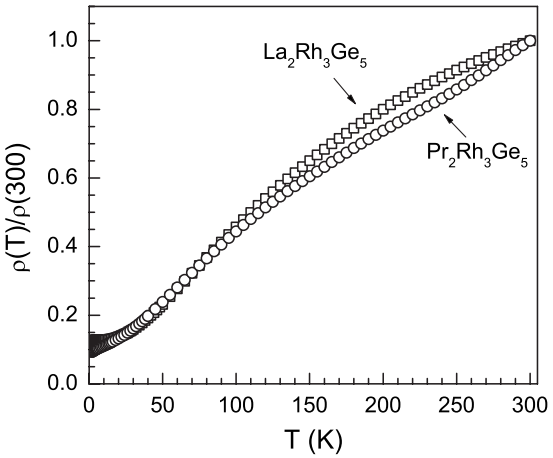

FIG. 7. Normalized electrical resistivity of $La_2Rh_3Ge_5$ and $Pr_2Rh_3Ge_5$ as a function of temperature in the temperature range 2–300 K.

glet CEF ground state.[12] The Sommerfeld coefficient γ in $Pr_2Rh_3Ge_5$ is enhanced and has a value of ~ 81 mJ/Pr mole K^2.

Figure 7 shows the electrical resistivity data of $La_2Rh_3Ge_5$ and $Pr_2Rh_3Ge_5$. The resistivity data of $La_2Rh_3Ge_5$ exhibit a very broad curvature around 150 K possibly due to the band effects together with a residual resistivity of ~ 39 $\mu\Omega$ cm (at 2 K) and a residual resistivity ratio of 9. A considerable departure from the linear temperature dependence is also observed in resistivity of $Pr_2Rh_3Ge_5$ on account of crystal field effects and/or band structure effects. The value of residual resistivity at 2 K is ~ 58 $\mu\Omega$ cm with the residual resistivity ratio of 11. The large residual resistivity is possibly due to the presence of (micro)cracks in the sample. In spite of the large residual resistivity in the sample, we made an attempt to extract the physics content in the data. The data at low temperature (below 4 K) fit to $\rho(T) = \rho_0 + AT^2$ with $A = 0.25874$ $\mu\Omega$ cm/K^2. This corresponds to $A/\gamma^2 = 3.94 \times 10^{-5}$ Ω cm K^2 mole^2 J^{-2}, which is larger than the universal value of Kadowaki–Woods ratio expected for the Ce-based Kondo lattice and/or heavy-fermion compounds.[18]

Furthermore, the Wilson ratio $R_W = 23.31$ using the value of $\chi = 0.106\,41$ emu/Pr mole at 2 K ($B = 0.1$ T) and $\gamma = 81$ mJ/Pr mole K^2 is also large similar to the case of non-Fermi-liquid heavy-fermion compound $YbRh_2Si_2$, which is situated very close to the quantum critical point in which a large Wilson ratio is attributed to the presence of ferromagnetic fluctuations.[19] Since the results obtained for $Pr_2Rh_3Ge_5$ are in the same range of the values, which are obtained for Ce- and Yb-based heavy-fermion systems, $Pr_2Rh_3Ge_5$ is a heavy-fermion system.

Since the electrical resistivity and specific heat data of $Pr_2Rh_3Ge_5$ do not show any signature of Kondo effect, the mechanism for the heavy-fermion behavior in $Pr_2Rh_3Ge_5$ is not the usual Kondo effect. Rather, the heavy-fermion behavior results from the low lying crystal field levels by the inelastic scattering of conduction electrons with the excited levels usually referred to as excitonic mass enhancement. The theory of excitonic mass enhancement was initially proposed by White and Fulde to explain the mass enhancement of Pr metal[20,21] and has recently been applied to explain the origin of heavy-fermion behavior in $PrOs_4Sb_{12}$.[6] There are two intrinsic requirements for the excitonic mass enhancement—the ground state must be a singlet and the splitting energy between the ground state and the first excited state must be low—to develop a heavy-fermion state. For our system $Pr_2Rh_3Ge_5$, both requirements are fulfilled—the ground state is nonmagnetic singlet and first excited state lies at 12 K—hence, $Pr_2Rh_3Ge_5$ is a heavy-fermion system that validates the theory of excitonic mass enhancement.

The magnetic and transport properties discussed above were reproduced in the second sample of $Pr_2Pd_3Ge_5$ and $Pr_2Rh_3Ge_5$, which establishes the intrinsic nature of the behavior.

IV. SUMMARY AND CONCLUSION

We synthesized and investigated two ternary compounds $Pr_2Pd_3Ge_5$ and $Pr_2Rh_3Ge_5$. In the case of $Pr_2Pd_3Ge_5$, the crystal field split ground state is doublet and the magnetization, electrical resistivity, and specific heat clearly establish that the compound orders antiferromagnetically below 8.3 K. It also shows unusually large magnetoresistance. $Pr_2Rh_3Ge_5$, on the other hand, has a singlet ground state and does not show any kind of order down to 0.5 K. A large value of Sommerfeld coefficient (81 mJ/mol K^2) is found in this compound. An enhanced Wilson ratio and an enhanced value of coefficient A together with large γ establish $Pr_2Rh_3Ge_5$ as a possible candidate for electronic mass enhancement due to low lying crystal field excitations. The role of low lying crystal field excitation for this enhanced Sommerfeld coefficient should be further explored by direct experimental verification of the crystal field level scheme and low lying excitations using inelastic neutron scattering.

*zakir@iitk.ac.in

[1] E. D. Bauer, N. A. Frederick, P.-C. Ho, V. S. Zapf, and M. B. Maple, Phys. Rev. B **65**, 100506(R) (2002).

[2] K. Izawa, Y. Nakajima, J. Goryo, Y. Matsuda, S. Osaki, H. Sugawara, H. Sato, P. Thalmeier, and K. Maki, Phys. Rev. Lett. **90**, 117001 (2003).

[3] Y. Aoki, A. Tsuchiya, T. Kanayama, S. R. Saha, H. Sugawara, H. Sato, W. Higemoto, A. Koda, K. Ohishi, K. Nishiyama, and R. Kadono, Phys. Rev. Lett. **91**, 067003 (2003).

[4] K. Kuwahara, K. Iwasa, M. Kohgi, K. Kaneko, N. Metoki, S. Raymond, M.-A. Méasson, J. Flouquet, H. Sugawara, Y. Aoki, and H. Sato, Phys. Rev. Lett. **95**, 107003 (2005).

[5] A. Yatskar, W. P. Beyermann, R. Movshovich, and P. C. Canfield, Phys. Rev. Lett. **77**, 3637 (1996).

[6] E. A. Goremychkin, R. Osborn, E. D. Bauer, M. B. Maple, N. A. Frederick, W. M. Yuhasz, F. M. Woodward, and J. W. Lynn, Phys. Rev. Lett. **93**, 157003 (2004).
[7] Z. Hossain, S. Hamashima, K. Umeo, T. Takabatake, C. Geibel, and F. Steglich, Phys. Rev. B **62**, 8950 (2000).
[8] M. Nakashima, H. Kohara, A. Thamizhavel, T. D. Matsuda, Y. Haga, M. Hedo, Y. Uwatoko, R. Settai, and Y. Ōnuki, J. Phys.: Condens. Matter **17**, 4539 (2005).
[9] V. K. Anand, A. K. Nandy, S. K. Dhar, C. Geibel, and Z. Hossain, J. Magn. Magn. Mater. **313**, 164 (2007).
[10] B. Becker, S. Ramakrishnan, D. Groten, S. Süllow, C. C. Mattheus, G. J. Nieuwenhuys, and J. A. Mydosh, Physica B (Amsterdam) **230-232**, 253 (1997).
[11] Z. Hossain, H. Ohmoto, K. Umeo, F. Iga, T. Suzuki, T. Takabatake, N. Takamoto, and K. Kindo, Phys. Rev. B **60**, 10383 (1999).
[12] S. Ramakrishnan, N. G. Patil, Aravind D. Chinchure, and V. R. Marathe, Phys. Rev. B **64**, 064514 (2001).
[13] E. Jobiliong, J. S. Brooks, E. S. Choi, H. Lee, and Z. Fisk, Phys. Rev. B **72**, 104428 (2005).
[14] C. Mazumdar, A. K. Nigam, R. Nagarajan, C. Godart, L. C. Gupta, B. D. Padalia, G. Chandra, and R. Vijayaraghavan, Appl. Phys. Lett. **68**, 3647 (1996).
[15] F. Tsui, C. Uher, and C. P. Flynn, Phys. Rev. Lett. **72**, 3084 (1994).
[16] N. Garcia, M. Muñoz, and Y.-W. Zhao, Phys. Rev. Lett. **82**, 2923 (1999).
[17] N. I. Solin and N. M. Chebotaev, Phys. Solid State **39**, 754 (1997).
[18] K. Kadowaki and S. B. Woods, Solid State Commun. **58**, 507 (1986).
[19] Y. Tokiwa, P. Gegenwart, T. Radu, J. Ferstl, G. Sparn, C. Geibel, and F. Steglich, Phys. Rev. Lett. **94**, 226402 (2005).
[20] R. M. White and P. Fulde, Phys. Rev. Lett. **47**, 1540 (1981).
[21] P. Fulde and J. Jensen, Phys. Rev. B **27**, 4085 (1983).